



THE CYTOTOXIC EFFECT OF USNIC ACID IN MALIGNANT MELANOMA CELLS WITH DIFFERENT GENOMIC PROFILES IN THE BRAF ASPECT

C. ÇOLAKOĞLU¹, A. HACİEFENDİ², İ.E. ERYILMAZ¹, G.G. ESKİLER², U. EGELİ¹, G. CECENER¹

¹Medical Biology Department, Bursa Uludag University, Faculty of Medicine, Bursa, Turkey

²Medical Biology Department, Sakarya University, Faculty of Medicine, Sakarya, Turkey

Abstract – Objective: Malignant melanoma (MM) is the most aggressive skin cancer and treatment options are still limited in the late stages, generally accompanied by BRAF mutations. Usnic acid (UA), a well-known traditional lichen metabolite, has a promising and selective antitumoral activity. However, the effects of UA on MM cells with different genomic profiles in the BRAF aspect have not been investigated yet. In this study, we evaluated the effect of UA on BRAF^{V600E} mutated-A2058 and wild-type MeWo cells.

Materials and Methods: In the UA-treated cells, viability and cell death analysis were performed by using WST-1 and Annexin-V assays. Then, the death-related morphological changes were visualized by acridine orange(AO)/ethidium bromide (EB) staining. The cell cycle regulatory effect of UA was determined. Finally, time-dependent detection of acidic vesicular organelles (AVOs) was performed by live-cell imaging.

Results: While MeWo viability significantly reduced to 53.8% and 28.6%, A2058 viability was detected as 61.3% and 50.3% at 50 and 100 μ M UA for 48 h. Thus, MeWo cells were found to be more sensitive to UA. Annexin-V and morphological analysis results showed that UA triggered mainly a vacuole-dependent cell death by the formation of AVOs, instead of apoptosis, in the MM cells. This effect was prominent in A2058 compared to MeWo. UA also slightly triggered apoptosis in MeWo cells. Thus, the cell cycle regulatory effect of UA on MM cells changed based on the cell death type triggered.

Conclusions: Our results suggest that UA exerts the cytotoxic effects on MM cells by inducing vacuole-dependent cell death, most probably autophagy, and the UA response of MM cells with a different genomic profile in the BRAF aspect varies.

KEYWORDS: Usnic acid, Malignant melanoma, Cytotoxic effect, BRAF mutation.

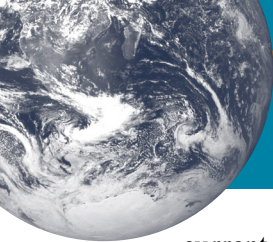
INTRODUCTION

The epidermis contains different cells like keratinocytes, Langerhans cells, and melanocytes. The cells localized in the basal layer of the epidermis and originating from neural crest cells are melanocytes¹. Their malignant transformation causes malignant melanoma (MM), the most aggressive

and deadliest form of skin cancer. Over the past few decades, MM incidence has increased, and it is predicted to increase further with depletion of the ozone layer and an increase in UV radiation. In the early stages, MM is mainly treated with surgery. However, treatment options are still limited in the late stages of the disease due to MM cells' high metastatic potency^{2,3}. Although



This work is licensed under a [Creative Commons Attribution-NonCommercial-ShareAlike 4.0 International License](https://creativecommons.org/licenses/by-nc-sa/4.0/)



current treatments include different options like chemotherapy, immunotherapy, photodynamic therapy or targeted therapies with specific inhibitors, MM treatment still faces several challenges such as therapy failures accompanied by the gene mutations, especially in *BRAF*, and side effects of the existing options. Therefore, novel therapeutic approaches are required for use in the treatment of MM⁴.

Natural products have been investigated for their therapeutic potentials in cancer, neurodegenerative and inflammatory diseases^{5,6}. Lichens are symbiotic microorganisms that synthesize a variety of secondary metabolites, including usnic acid (UA)^{7,8}. UA is a well-known traditional lichen compound with anti-tumorigenic, antioxidant, anti-inflammatory, antiproliferative activities in various cancer cells⁹. Besides these properties, UA has been characterized as an apoptotic or autophagic inducer in different cancer cells by type and stage-dependent¹⁰. Moreover, promising selective cytotoxic and anti-invasive effects of UA have been evaluated on the *BRAF* and *NRAS* wild-type HTB-140 (Hs 294T)- human melanoma cells and exert strong inhibitory effects on the proliferation of cancer cells¹¹. However, UA's selective cytotoxic effect on MM cells with different genomic profiles, especially in the *BRAF* aspect, has not been investigated in the literature. Thus, we aimed to evaluate the possible changes in the UA response of two different MM cell lines based on the oncogenic peculiarity and genomic features of the cells by selecting the MM cell lines as more aggressive A2058 with *BRAF*^{V600E} mutation (*BRAF*^{V600E}, *NRAS*^{WT}, *PTEN*^{null}) and less aggressive MeWo (*PTEN*-proficient *BRAF* and *NRAS* wild-type) cells, after treatment with different concentrations of UA, as an apoptotic or autophagic inducer, for the first time.

MATERIALS AND METHODS

Cell Lines and Chemicals

The human MM cell lines A2058 (*BRAF*^{V600E} mutated) (CRL-11147TM) and MeWo (HTB-65TM) (*BRAF* wild-type) were purchased from American Type Culture Collection (ATCC, Manassas, VA, USA). UA ($\geq 98\%$ purity) and acridine orange as powder forms, and ethidium bromide were purchased from Sigma-Aldrich (St Louis, MO, USA) and prepared in 0.01% dimethyl sulfoxide (DMSO) solution before cell culture applications as previously described¹². WST-1 Cell Proliferation Kit was purchased from BioVision (San Francisco, CA, USA). Dulbecco's Modified

Eagle medium (DMEM), 4.5 g/l D-glucose, sodium pyruvate, and L-glutamine, Trypsin-EDTA 0.25%, antibiotic-antimycotic, and MEM non-essential amino acid solutions were purchased from Thermo Fisher Scientific (Waltham, MA, USA). Muse[®] Annexin V and Dead Cell Assay Kit, Cell Cycle Assay Kit, DMSO, ethanol, and 4% paraformaldehyde solutions were obtained from Luminex (Austin, TX, USA).

Cell Culture Conditions

A2058 cell lines were cultured in DMEM containing sodium pyruvate, 4.5 g/l D-glucose, and L-glutamine and supplemented with 10% FBS, and 1% antibiotic-antimycotic solution. MeWo cell lines were cultured in DMEM supplemented with 10% FBS, 1% antibiotic-antimycotic and 1% MEM non-essential amino acid solutions. Cell lines were incubated at 37°C in a humidified atmosphere of 95% air and 5% CO₂. Medium changed every 2-3 days, and the cells were subcultured by trypsinization when their confluency reached 80%.

Cell Viability Test

The UA-treated cells' viability was determined by WST-1 Cell Proliferation Kit protocol. Briefly, A2058 and MeWo cells were seeded into 96-well plates at a density of 2×10^4 cells/well in a 100 μ l growth medium for overnight incubation. The seeded cells were treated with five different doses of UA, 12.5, 25, 50, 75, and 100 μ M, for 24 and 48 h. After the indicated times, 10 μ l WST-1 reagent was added to each well, and the cells were incubated for approximately 2 h at 37°C and 5% CO₂. Then, absorbance measurement was performed at 450 nm using a TriStar² LB 942 monochromator microplate reader (Berthold Technologies, Bad Wildbad, Germany). All measurements were performed in triplicate. IC₅₀ values of UA for MeWo and A2058 were determined as 62.8 and 89.8 μ M, respectively. Based on the cell viability results, the following experiments were performed with only two different concentrations of UA (50 and 100 μ M) due to the different responses of the cells.

Determination of the Apoptotic Effect

The apoptotic effects of UA on A2058 and MeWo cells were analyzed according to the Muse[®] Annexin V and Dead Cell Assay Kit (Luminex, Austin, TX, USA) protocol. The cells were cultured

into 6-well plates at a density of 1×10^5 cells/well and treated with 50 and 100 μM of UA for 48 h. At the end of the time, the cells were harvested by trypsinization and washed twice with PBS. Then, the cells' pellet was stained with Annexin V - Dead Cell Assay Kit reagent for 30 min in the dark. Detection was performed in a Muse[®] Cell Analyzer (Luminex, Austin, TX, USA).

Cell Cycle Analysis

The effects of UA on cell cycle regulation on MM cells were analyzed according to the Muse[®] Cell Cycle Assay Kit (Luminex, Austin, TX, USA) protocol. The cells were seeded into 6-well plates at a density of 1×10^6 cells/well and treated with 50 and 100 μM of UA. The treated cells were fixed in a cold 70% EtOH solution and stored at -20°C for 3 h. The fixed-cell pellets were collected by centrifugation and then stained with a Cell Cycle reagent for 30 min in the dark. Detection was performed in a Muse[®] Cell Analyzer (Luminex, Austin, TX, USA).

Acridine Orange/Ethidium Bromide Staining

Acridine orange/ethidium bromide (AO/EB) staining was used to visualize death-related morphological changes in the UA-treated MM cells. Briefly, A2058 and MeWo cells were seeded into 6-well plates at a density of 5×10^5 and treated with 50 and 100 μM UA for 48 h. The treated cells were fixed using a 4% paraformaldehyde solution. After washing twice with cold PBS, the cells were stained with AO/EB solution and visualized under an EVOS FL Cell Imaging System (Waltham, MA, USA).

Detection of Acidic Vesicular Organelles (AVOs)

We also performed live-cell staining by AO to detect AVOs, which are characteristics of autophagy¹³. The stock solution of AO in 10 ml PBS was prepared and stored in appropriate conditions. The cells seeded into 6-well plates at a density of 5×10^5 were treated with 50 and 100 μM UA for 12, 18, 24, and 36 h. At the end of each incubation time, the cells were washed with PBS and stained with 1 $\mu\text{g}/\mu\text{l}$ AO solution for 15 min. After washing cells twice with PBS, AVOs were determined under an EVOS FL Cell Imaging System (Waltham, MA, USA).

Statistical Analysis

Statistical analysis was performed with GraphPad Prism 6 (La Jolla, CA, USA). The results were replicated three times and expressed as mean \pm SD. The difference between groups was determined using an analysis of variance (ANOVA) determination with an appropriate post-hoc test. Statistical significance was accepted when the p -values were lower than 0.05.

RESULTS

Cytotoxic Effect of UA on MM Cells

For determining the cytotoxic effect, MM cells were treated with the increasing concentrations of UA for 24 and 48 h and analyzed using WST-1 proliferation assay. As shown in Figure 1, UA caused a significant reduction in the cell viability percentages of MeWo and A2058 MM cells in a time- and dose-dependent manner (** $p < 0.01$). However, UA triggered more reduction in the proliferation of *BRAF* wild-type MeWo cells than those of *BRAF*^{V600E} mutated A2058 cells. While the UA-treated A2058 viability ratios were detected as 61.3% and 50.3% at 50 and 100 μM UA, respectively for 48 h (** $p < 0.01$; Figure 1a), UA-treated MeWo viability significantly reduced to 53.8% and 28.6%, respectively (** $p < 0.01$; Figure 1b). Therefore, we determined that UA treatment was more effective on the *BRAF* wild-type MM cells, MeWo. The subsequent experiments were performed with only two different concentrations of UA, 50 and 100 μM .

Apoptotic Effect of UA on MM Cells

Annexin V analysis was performed to evaluate the apoptotic effects of UA on MM cells for 48 h. As shown in the plots (Figure 2a), UA did not induce apoptotic cell death in *BRAF*^{V600E} mutated A2058 cells at both 50 and 100 μM treatments. Similarly, 50 μM UA treatment did not trigger apoptosis in *BRAF* wild-type MeWo cells. However, 100 μM UA increased the total apoptotic MeWo cells to 27.6% compared with the control group (Figure 2b). However, these results were not statistically significant ($p > 0.05$). Thus, we concluded that UA did not induce significant apoptosis in both MM cells, except a slight increase in apoptotic cell death in *BRAF* wild-type MeWo cells, compared to *BRAF*^{V600E} mutated A2058 cells, at 100 μM concentration.

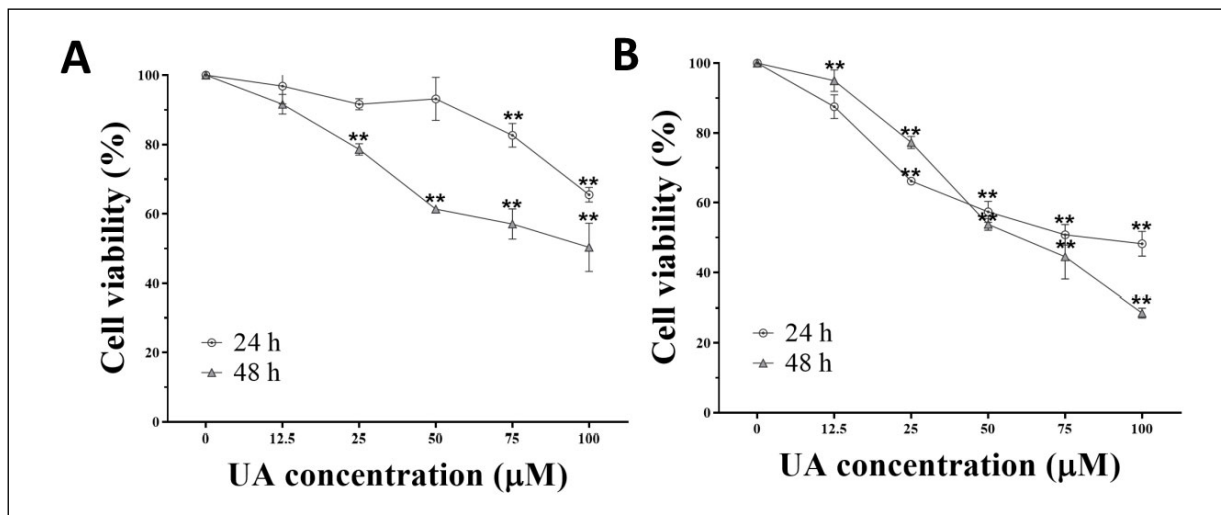


Figure 1. Cell viability percentages in (A) *BRAF*^{V600E} mutated A2058 and (B) *BRAF* wild-type MeWo cells after UA treatment for 24 and 48 h (***p*<0.01).

Cell Cycle Regulatory Effect of UA on MM Cells

We also performed the analysis to detect the cell cycle regulatory effect of UA on the MM cells. We found that UA triggered cell cycle arrest at G0/G1 phase in *BRAF*^{V600E} mutated A2058 cells.

The percentage of A2058 cells in the G0/G1 phase increased from 48.7% to 60.6% at 100 μM for 48 h (Figure 3a). However, UA did not show any considerable effect on *BRAF* wild-type MeWo cells, as shown in Figure 3b. Thus, UA differently affected cell cycle regulation in these MM cells.

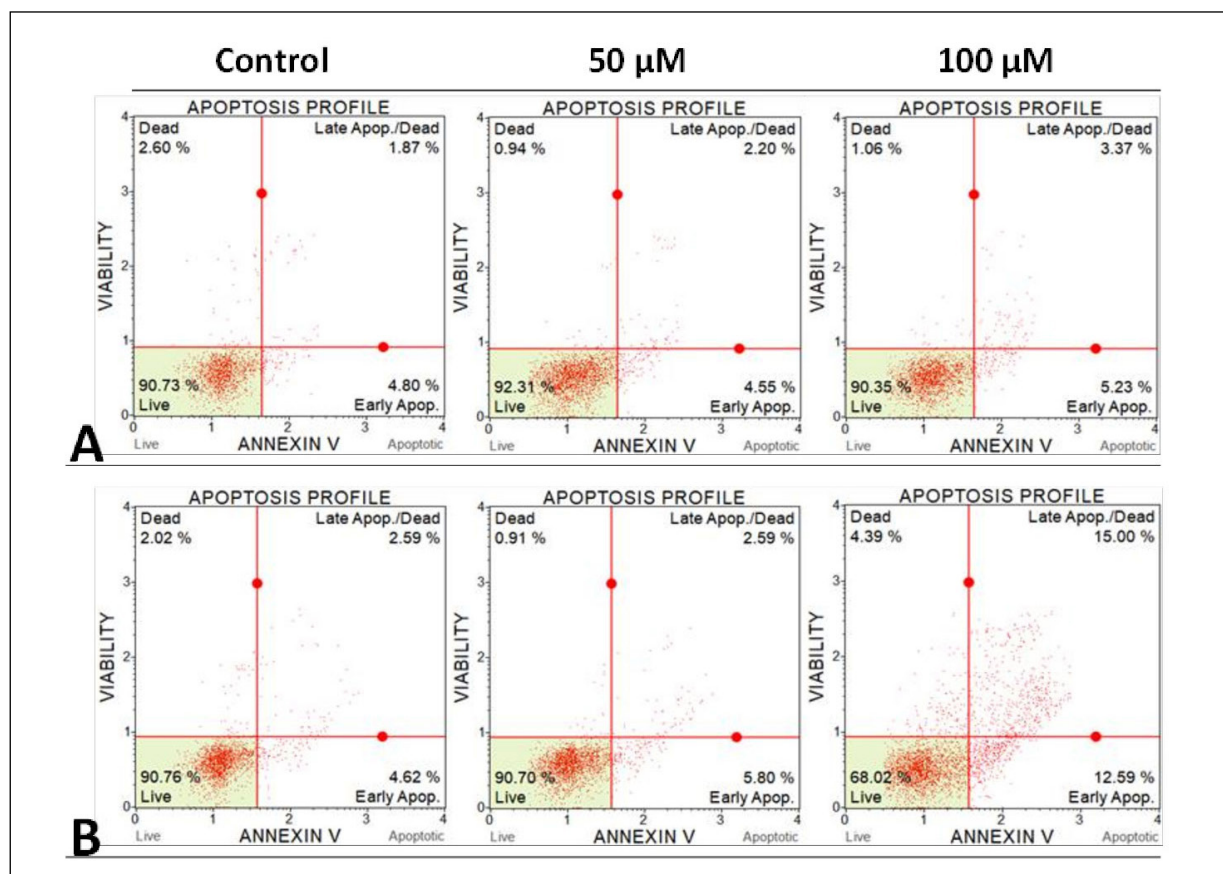


Figure 2. Total apoptotic cells percentages in (A) *BRAF*^{V600E} mutated A2058 and (B) *BRAF* wild-type MeWo cells after UA treatment for 48 h.

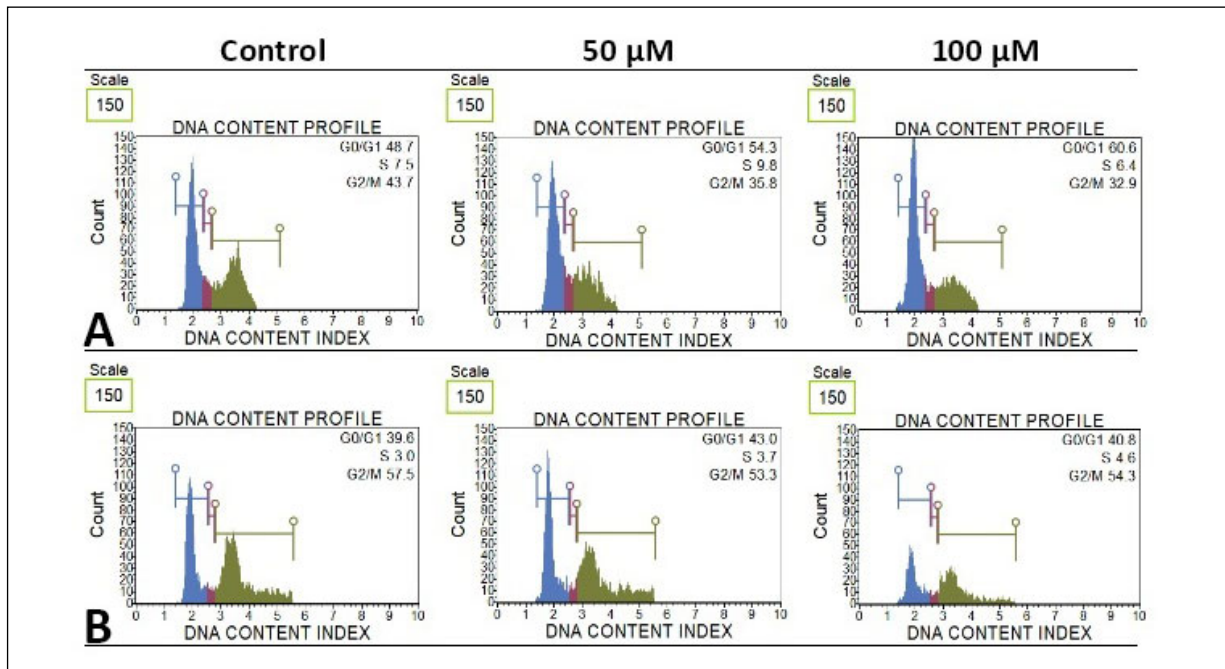


Figure 3. Effect of UA on cell cycle progression in (A) *BRAF*^{V600E} mutated A2058 and (B) *BRAF* wild-type MeWo cells after UA treatment for 48 h.

Effects of UA on the Cell Morphology

We performed AO/EB staining to visualize the death-related morphological changes of the UA-treated MM cells. UA increased the number of cellular vacuolization in a dose-dependent manner, and 100 μM UA caused a noticeable increase in the number and size of vacuoles, especially in *BRAF*^{V600E} mutated A2058 cells, as observed in

Figure 4a. Similarly, 50 μM UA treatment also induced the accumulation of vacuoles in *BRAF* wild-type MeWo cells. However, the observed vacuoles in MeWo cells were smaller and fewer than those of A2058, especially at 50 μM UA treatment. Moreover, some apoptotic cells were also observed in response to 100 μM UA treatment in MeWo cells (Figure 4b). Therefore, the results of morphological changes detected in UA-treated MM cells, support-

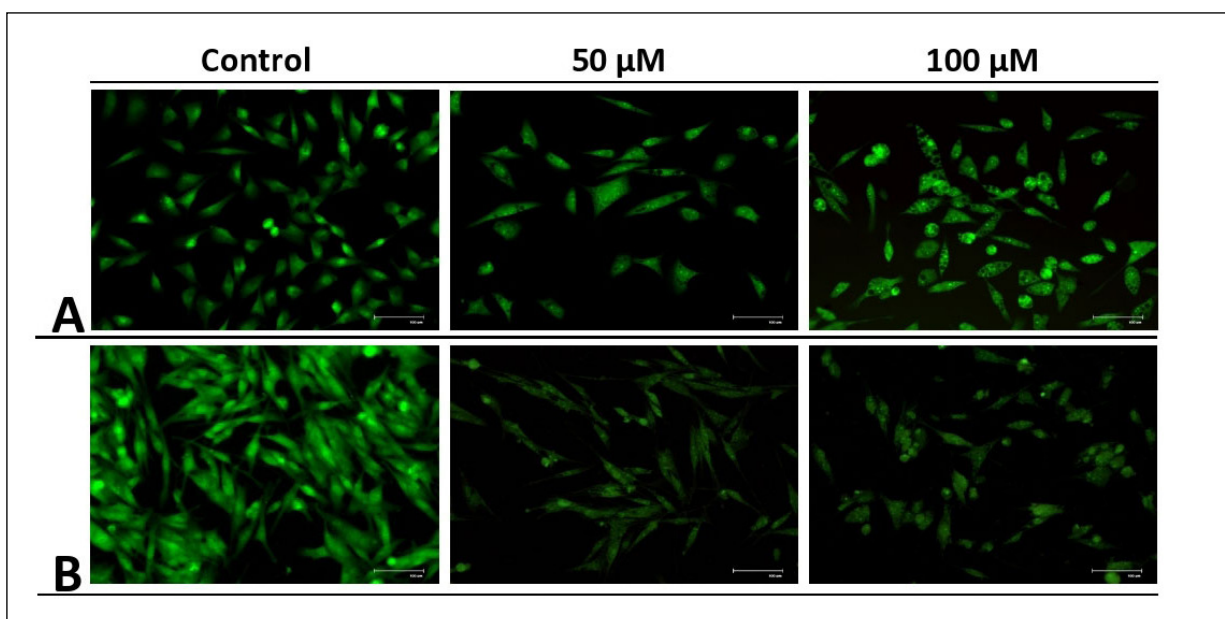


Figure 4. The morphological changes of UA on MM cell lines. (A) *BRAF*^{V600E} mutated A2058 and (B) *BRAF* wild-type MeWo cells after treatment with increasing concentrations of UA for 48 h.



ed by WST-1 and Annexin V results, indicated that UA induced vacuole-dependent cell death, instead of apoptosis, in particularly *BRAF*^{V600E} mutated A2058 cells.

Effect of UA on AVOs Formation in MM Cells

Live-cell staining with AO was performed for detection of AVOs formation that is a characteristic for autophagy, a major vacuole-dependent cell

death, in the UA-treated MM cells for 12, 18, 24, and 36 h. Our result showed that AVOs formation was observed in both MM cells after UA treatments. While AVOs were increased in a dose-dependent manner as observed for 12, 18, and 24 h, the red fluorescence decreased for 36 h UA treatment in *BRAF*^{V600E} mutated A2058 MM cells (Figure 5). Additionally, AVOs positive cells increased in a dose-dependent manner for 24 and 36 h in *BRAF* wild-type MeWo MM cells (Figure 6). These results were consistent with the morphological changes of the cells after UA treatment.

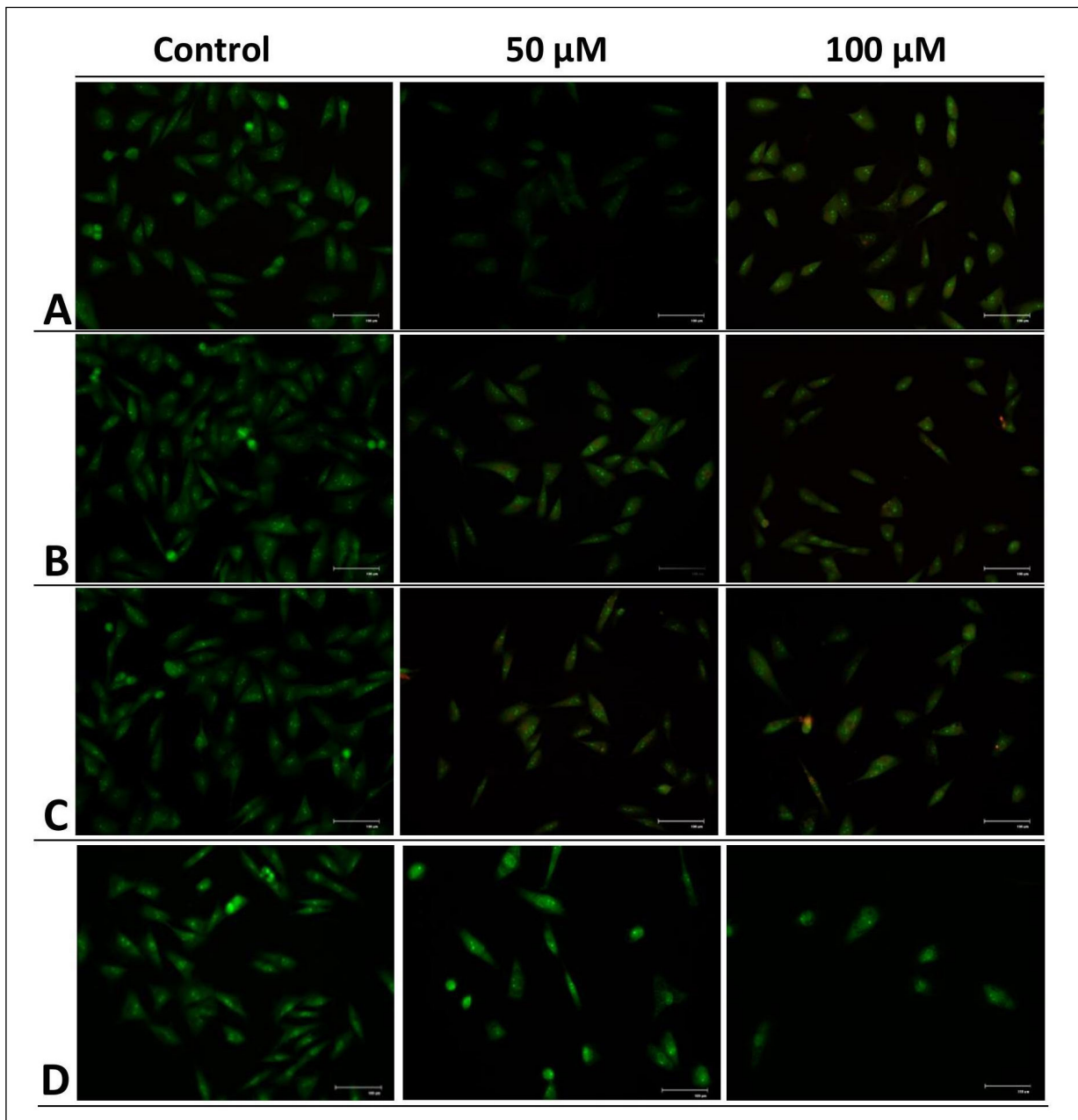


Figure 5. The live-cell imaging results of *BRAF*^{V600E} mutated A2058 cells. The cells were treated with 50 and 100 μ M UA for (A) 12 h (B) 18 h (C) 24 h (D) 36 h. AVOs formation which was observed as red fluorescence increased following treatment with increasing concentration of UA, especially at 12, 18 and 24 h.

Thus, we concluded that UA induced an acidic vacuole-dependent cell death, most probably autophagy due to UA's known autophagic inducer effect in both MM cells.

DISCUSSION

Malignant melanoma (MM), the deadliest form of skin cancer that develops due to the malignant transformation of melanocytes, shows rapid progression with high metastatic properties¹⁴. MM is

treated with surgery in the earlier stages. However, treatment options are still limited after progression¹⁵. One of the molecular alterations that complicate MM therapy in the later stages is the presence of *BRAF*^{V600E} mutation. *BRAF*-mutated-MMs exhibit more aggressive features compared with wild-type ones¹⁶. Thus, there is a need for new therapeutic candidates for effective treatment of MM, especially *BRAF*-mutated ones.

Usnic acid (UA) is a natural active compound derivative of dibenzofuran, synthesized as a secondary metabolite in lichens¹⁷. Although the anti-

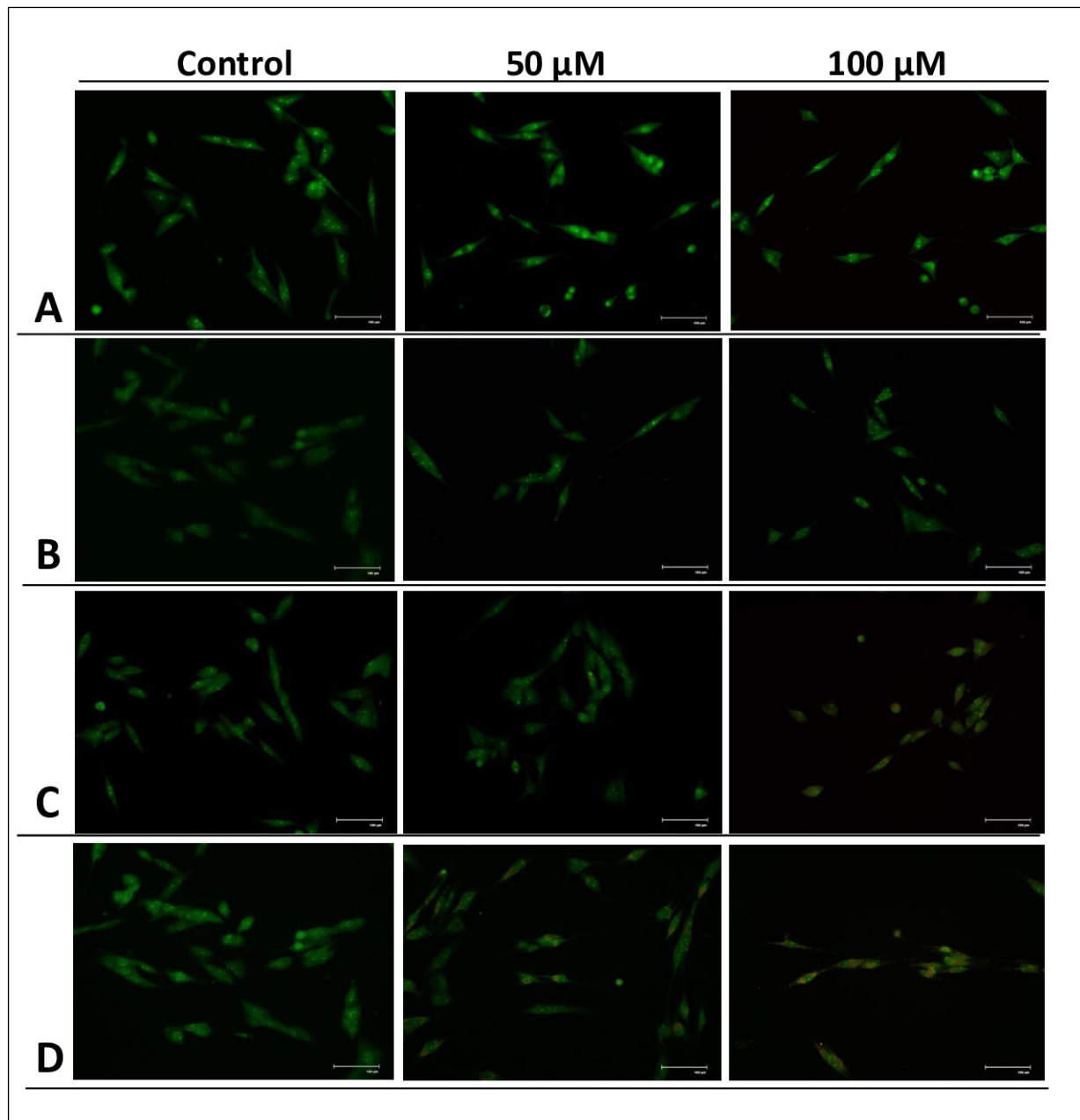


Figure 6. The live-cell imaging results of *BRAF* wild-type MeWo cells. The cells were treated with 50 and 100 μ M UA for (A) 12 h (B) 18 h (C) 24 h (D) 36 h. AVOs formation which was observed as red fluorescence increased following treatment with increasing concentration of UA, especially at 24 and 36 h.



tumoral effects of UA have been widely studied in several types of cancer, including MM, UA's cytotoxic effect on MM cells with different genomic profiles in the *BRAF* aspect has not been investigated yet. Therefore, in the current study, we evaluated the promising effects of UA on the different MM cell lines, A2058 and MeWo, based on the genomic profile in the *BRAF* aspect.

Our results showed that UA caused a significant reduction in the viability of both MM cells. However, *BRAF* wild-type MeWo cells were more sensitive to UA treatments than A2058 cells with *BRAF*^{V600E} mutation. Furthermore, we determined that UA triggered vacuole-dependent cell death in both cells through the detection of AVO formation. However, its effect was more profound in *BRAF*^{V600E} mutated-A2058. These results were consistent with the Annexin V analysis results, showing that a higher concentration of UA treatment resulted in apoptotic cell death in *BRAF* wild-type MeWo cells. Additionally, UA treatment caused a significant increase in G0/G1 arrest of A2058 cells, unlike MeWo cells. Therefore, our findings showed that UA mediated apoptotic or probably autophagic activity based on the *BRAF* status of MM cells.

UA has been reported as an autophagy and apoptosis inducer in cancer cells, depending on concentrations, exposure times, and types of the cancer cells¹⁸⁻²¹. Our previous study has shown that UA treatment induced both apoptosis and autophagy in hepatocellular carcinoma, and its activity changed by HBV infection dependent¹⁰. However, we previously found that UA induced only apoptotic cell death in hormone-dependent breast and prostate cancer cells¹². Additionally, recent studies indicated that autophagy activation is induced by inhibition of apoptotic cell death, inactivating mammalian target of rapamycin (mTOR), and activating c-Jun N-terminal kinases (JNK) during UA-induced cytotoxicity²¹⁻²³. Moreover, *BRAF* is a member of the mitogen-activated protein kinase (MAPK) signal transduction cascade. The *BRAF*^{V600E} is the most common *BRAF* mutation in MM, which is responsible for the refractory MM phenotype²⁴. Oncogenic *BRAF* mutation is associated with the induction of chronic ER stress, which results in an increased basal level of autophagy and apoptotic resistance in cutaneous melanoma. Thus, the induction of autophagy could be related to the inhibition of apoptosis in the cells^{25,26}. Moreover, in the late stages of cancer, autophagy is defined as a cytoprotective process for the survival of cancer cells²⁷. As consistent with the literature findings, our results showed that UA induced vacuole-dependent cell death, most probably autophagy, not apoptosis,

in the *BRAF*^{V600E} mutated-A2058 MM cells at especially 100 μ M UA, suggesting that *BRAF*^{V600E} mutation could contribute to preventing apoptosis and decreasing UA sensitivity of A2058 cells. In addition, in the *BRAF* wild-type MeWo cells, UA triggered less AVOs formation, especially at 100 μ M, and induced more apoptotic cell death, unlike A2058 cells. Similarly, as indicated in the literature, *BRAF*^{V600E} mutation increase autophagy induction in central nervous system (CNS) tumors compared to the wild-type CNS cells²⁸. Therefore, our results were also consistent with the findings that *BRAF*^{V600E}-mutated A2058 cells were less sensitive to UA treatment than the *BRAF* wild-type MeWo cells.

Moreover, in the *BRAF*^{V600E} mutated-A2058 cells, UA induced G0/G1 cell cycle arrest and cell death induction. However, UA did not show any considerable effect on the cell cycle regulation in the *BRAF* wild-type MeWo cells. The previous studies indicated that, while UA induced G0/G1 phase arrest in gastric cancer, G2/M phase arrest was also observed in the UA-treated AGS gastric cancer cells, accompanied by UA-triggered apoptosis or autophagy. UA also causes G0/G1 cell cycle arrest by decreasing the expression of CDK4, CDK6, and cyclin D1 and increasing the p21/cip1 protein expression in lung cancer. Our previous results have shown that UA treatment induces p53-mediated apoptosis in breast and prostate cancer cells by causing cell cycle arrest in G0/G1 phase^{18,21}. In addition, everolimus, an mTOR inhibitor, causes the induction of autophagy through G0/G1 cell cycle arrest and degradation of cyclin D1 in breast cancer cells. However, G2/M phase arrest could also co-occur with the induction of autophagy, as in the artesunate-treated breast cancer cells²⁹⁻³¹. These results suggest that cell cycle progression could be regulated by autophagy or apoptosis induction at different phases, as in our study. After UA treatment, induction of vacuole-dependent cell death stimulated the arrest of the cell cycle in the G0/G1 phase in the *BRAF*^{V600E} mutated-A2058 cells. However, UA did not cause a significant alteration in the cell cycle regulation on *BRAF* wild-type MeWo cells, suggesting that the induction of two different types of cell death by UA could differentially affect cell cycle regulation at different phases by depending on MM cells' genomic profiles.

CONCLUSIONS

Our results indicated that UA exerted a variable cytotoxic effect on the MM cells by inducing different types of cell death based on the genomic

profiles of the cells in the *BRAF* aspect. As a limitation of this study, next studies should focus on the detailed molecular mechanisms underlying the UA-triggered cell death activation by the formation of AVOs in the *BRAF*-mutated MM cells for revealing whether this type of cell death represents a defense mechanism that prevents apoptosis against UA-triggered cytotoxicity in these MM cells in the *BRAF* aspect.

FINANCIAL SUPPORT:

The authors received no financial support for the research.

ETHICAL COMMITTEE:

The study was conducted according to the Institutional requirements and Helsinki Declaration.

CONFLICT OF INTEREST:

The authors declare that they have no conflict of interest.

REFERENCES

- Bandarchi B, Ma L, Navab R, Seth A, Rasty G. From melanocyte to metastatic malignant melanoma. *Dermatol Res Pract* 2010; 2010: 583748.
- Carr S, Smith C, Wernberg J. Epidemiology and Risk Factors of Melanoma. *Surg Clin North Am* 2020; 100: 1-12.
- Domingues B, Lopes JM, Soares P, Populo H. Melanoma treatment in review. *Immunotargets Ther* 2018; 7: 35-49.
- Ny L, Hernberg M, Nyakas M, Koivunen J, Oddershede L, Yoon M, Wang X, Guyot P, Geisler J. BRAF mutational status as a prognostic marker for survival in malignant melanoma: a systematic review and meta-analysis. *Acta Oncol* 2020; 59: 833-844.
- Houghton PJ, Howes MJ. Natural products and derivatives affecting neurotransmission relevant to Alzheimer's and Parkinson's disease. *Neurosignals* 2005; 14: 6-22.
- Molnár K, Farkas E. Current results on biological activities of lichen secondary metabolites: a review. *Z Naturforsch C J Biosci* 2010; 65: 157-73.
- Cetin Cakmak K, Gülçin İ. Anticholinergic and antioxidant activities of usnic acid-an activity-structure insight. *Toxicol Rep* 2019; 6: 1273-1280.
- Thadhani VM, Karunaratne V. Potential of Lichen Compounds as Antidiabetic Agents with Antioxidative Properties: A Review. *Oxid Med Cell Longev* 2017; 2017: 2079697.
- Qi W, Lu C, Huang H, Zhang W, Song S, Liu B. (+)-Usnic Acid Induces ROS-dependent Apoptosis via Inhibition of Mitochondria Respiratory Chain Complexes and Nrf2 Expression in Lung Squamous Cell Carcinoma. *Int J Mol Sci* 2020; 21: 2915.
- Yurdacan B, Egeli U, Eskiler GG, Eryilmaz IE, Cecener G, Tunca B. The role of usnic acid-induced apoptosis and autophagy in hepatocellular carcinoma. *Hum Exp Toxicol* 2019; 38: 201-215.
- Galanty A, Koczurkiewicz P, Wnuk D, Paw M, Karnas E, Podolak I, Węgrzyn M, Borusiewicz M, Madeja Z, Czyż J, Michalik M. Usnic acid and atranorin exert selective cytostatic and anti-invasive effects on human prostate and melanoma cancer cells. *Toxicol In Vitro* 2017; 40: 161-169.
- Eryilmaz IE, Guney Eskiler G, Egeli U, Yurdacan B, Cecener G, Tunca B. In vitro cytotoxic and antiproliferative effects of usnic acid on hormone-dependent breast and prostate cancer cells. *J Biochem Mol Toxicol* 2018; 32: e22208.
- Thomé MP, Filippi-Chiela EC, Villodre ES, Migliavaca CB, Onzi GR, Felipe KB, Lenz G. Ratiometric analysis of Acridine Orange staining in the study of acidic organelles and autophagy. *J Cell Sci* 2016; 129: 4622-4632.
- Lodde G, Zimmer L, Livingstone E, Schadendorf D, Ugurel S. Malignes Melanom [Malignant melanoma]. *Hautarzt* 2020; 71: 63-77.
- Ahmed B, Qadir MI, Ghafoor S. Malignant Melanoma: Skin Cancer-Diagnosis, Prevention, and Treatment. *Crit Rev Eukaryot Gene Expr* 2020; 30: 291-297.
- Czarnecka AM, Bartnik E, Fiedorowicz M, Rutkowski P. Targeted Therapy in Melanoma and Mechanisms of Resistance. *Int J Mol Sci* 2020; 21: 4576.
- Cansaran-Duman D, Tanman Ü, Yangin S, Atakol O. The comparison of miRNAs that respond to anti-breast cancer drugs and usnic acid for the treatment of breast cancer. *Cytotechnology* 2020; 72: 855-872.
- Singh N, Nambiar D, Kale RK, Singh RP. Usnic acid inhibits growth and induces cell cycle arrest and apoptosis in human lung carcinoma A549 cells. *Nutr Cancer* 2013; 65: 36-43.
- Değerli E, Torun V, Cansaran-Duman D. miR-185-5p response to usnic acid suppresses proliferation and regulating apoptosis in breast cancer cell by targeting Bcl2. *Biol Res* 2020; 53: 19.
- Krajka-Kuźniak V, Paluszczak J, Kleszcz R, Baer-Dubowska W. (+)-Usnic acid modulates the Nrf2-ARE pathway in FaDu hypopharyngeal carcinoma cells. *Mol Cell Biochem* 2021; 476: 2539-2549.
- Geng X, Zhang X, Zhou B, Zhang C, Tu J, Chen X, Wang J, Gao H, Qin G, Pan W. Usnic Acid Induces Cycle Arrest, Apoptosis, and Autophagy in Gastric Cancer Cells In Vitro and In Vivo. *Med Sci Monit* 2018; 24: 556-566.
- Chen S, Dobrovolsky VN, Liu F, Wu Y, Zhang Z, Mei N, Guo L. The role of autophagy in usnic acid-induced toxicity in hepatic cells. *Toxicol Sci* 2014; 142: 33-44.
- Ebrahim HY, Akl MR, Elsayed HE, Ronald AH, El Sayed KA. Usnic acid benzylidene analogues as potent mechanistic target of rapamycin inhibitors for the control of breast malignancies. *J Nat Prod* 2017; 80: 932-952.
- Luebker SA, Koepsell SA. Diverse Mechanisms of BRAF Inhibitor Resistance in Melanoma Identified in Clinical and Preclinical Studies. *Front Oncol* 2019; 9: 268.
- Rather RA, Bhagat M, Singh SK. Oncogenic BRAF, endoplasmic reticulum stress, and autophagy: Crosstalk and therapeutic targets in cutaneous melanoma. *Mutat Res Rev Mutat Res* 2020; 785: 108321.
- Gump JM, Thorburn A. Autophagy and apoptosis: what is the connection? *Trends Cell Biol* 2011; 21: 387-392.
- Yang ZJ, Chee CE, Huang S, Sinicrope FA. The role of autophagy in cancer: therapeutic implications. *Mol Cancer Ther* 2011; 10: 1533-1541.
- Levy JM, Thompson JC, Griesinger AM, Amani V, Donson AM, Birks DK, Morgan MJ, Mirsky DM, Handler MH, Foreman NK, Thorburn A. Autophagy inhibition improves chemosensitivity in BRAF(V600E) brain tumors. *Cancer Discov* 2014; 4: 773-780.
- Guney Eskiler G, Eryilmaz IE, Yurdacan B, Egeli U, Cecener G, Tunca B. Synergistic effects of hormone therapy drugs and usnic acid on hormone receptor-positive breast and prostate cancer cells. *J Biochem Mol Toxicol* 2019; 33: e22338.



30. Chen G, Ding XF, Bouamar H, Pressley K, Sun LZ. Everolimus induces G1 cell cycle arrest through autophagy-mediated protein degradation of cyclin D1 in breast cancer cells. *Am J Physiol Cell Physiol* 2019; 317: C244-C252.
31. Chen K, Shou LM, Lin F, Duan WM, Wu MY, Xie X, Xie YF, Li W, Tao M. Artesunate induces G2/M cell cycle arrest through autophagy induction in breast cancer cells. *Anticancer Drugs* 2014; 25: 652-662.